

Full Articles

Quantum chemical study of the mechanism of catalytic [2+2+2] cycloaddition of acrylic acid esters to norbornadiene in the presence of nickel(0) complexes*

R. S. Shamsiev* and V. R. Flid

M. V. Lomonosov Moscow State University of Fine Chemical Technology,
86 prosp. Vernadskogo, 119571 Moscow, Russian Federation.
Fax: +7 (495) 434 8711. E-mail: Shamsiev.R@gmail.com

The mechanism of the [2+2+2] cycloaddition of ethyl acrylate to norbornadiene (NBD) catalyzed by Ni⁰ complexes was modeled in terms of the density functional theory (DFT) at the PBE level. The formation of the first C—C bond between the coordinated NBD and ethyl acrylate molecules is the rate-determining step of the process. The low stereoselectivity of the reaction is due to the close matching of the activation barriers for the formation of *exo*- and *endo*-cycloadducts (25.6 and 24.9 kcal mol⁻¹, respectively).

Key words: reaction mechanism, nickel intermediates, cycloaddition, norbornadiene, acrylates, density functional theory (DFT), PBE functional.

Catalytic processes involving bicyclo[2.2.1]hepta-2,5-diene or norbornadiene (NBD) offer exceptional possibilities for the synthesis of difficult to obtain polycyclic compounds¹ with unique properties (high density, high specific heat of combustion, and so on). Polycyclic compounds based on NBD hold promise as motor fuel additives,^{2,3} as well as for the modification of rubbers.

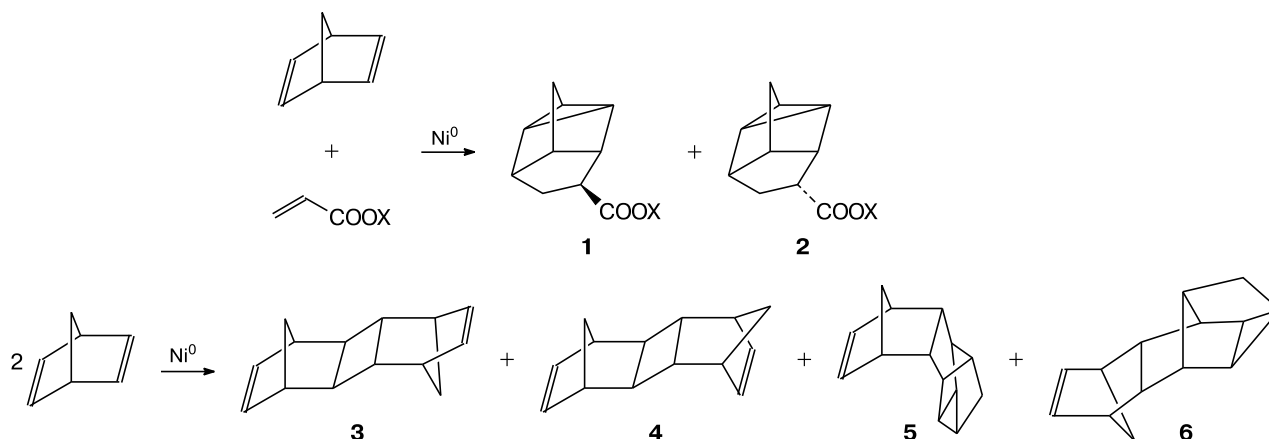
Due to specific features of the molecular structure of NBD, its cycloaddition reactions have limitless possibilities for studying and achieving different directions and

levels of isomerization. Complexes of Ni⁰ catalyze various reactions involving NBD, in particular, its cycloaddition to activated olefins. The coordination mode of NBD and olefin molecules to the Ni atom, as well as the composition and structures of the key intermediates, determine the stereochemistry and the ratio of the reaction products.

The reaction of NBD with acrylic acid esters has a general character and affords *exo* and *endo* stereoisomers (**1** and **2**) of [2+2+2] cycloadducts of olefins with NBD, as well as various [2+2] and [2+2+2] homodimers of NBD (**3–6**)^{4–6} (Scheme 1). A system based on Ni(C₃H₅)₂, which generates catalytically active Ni⁰ complexes in the presence of NBD, was used as the catalyst.

* Dedicated to Academician of the Russian Academy of Sciences M. P. Egorov on the occasion of his 60th birthday.

Scheme 1



Both reactions are described by second-order kinetic equations:

$$dC_{\text{prod}}/dt = W_I = k_{\text{obs}}C(\text{Ni})C(\text{olefin}),$$

$$dC_{\text{dim}}/dt = W_{II} = k_{\text{obs}}C(\text{Ni})C(\text{NBD}).$$

The reaction rate depends on the structure of the olefin used. The ratios of the stereoisomers for the first and second reactions remain unchanged in the course of the experiment and depend only on the solvent and the nature of acrylate. The kinetic data provide evidence that different stereoisomers are produced from the same key intermediates by parallel-pathways.⁶

Kinetic experimental data are not sufficient to determine the quantitative characteristics of equilibrium steps of interconversions of the intermediates. Therefore, it was important to study the mechanism of this process by quantum chemical methods.

In the present study, we report the results of the quantum chemical modeling of the reaction mechanism of the formation of the *exo*- and *endo*-[2+2+2] cycloadducts of ethyl acrylate (EA) with NBD catalyzed by nickel complexes.

Calculation procedure

Calculations were carried out in terms of the density functional theory (DFT) using the PRIRODA program⁷ with the non-empirical PBE exchange-correlation functional⁸ and the TZ2P basis set. This approach has been employed earlier to calculate nickel complexes⁹ and the mechanism^{10,11} of [2+2] cyclodimerization of NBD catalyzed by Ni^I complexes. The following Gaussian basis sets (non-contracted/contracted) were used: (5s1p)/[3s1p] for H atoms, (11s6p2d)/[6s3p2d] for C atoms, and (17s13p8d)/[12s9p4d] for Ni atoms.

The geometry optimization for the molecule was performed without symmetry constraints. The types of stationary points were determined based on the analytically computed second derivatives of the energy and vibrational frequencies. To verify the direct relationship between the determined transition states (TS) and local minima, we performed intrinsic reaction coordinate

(IRC) calculations. The Gibbs free energies were calculated for 323 K. The solvation effects (toluene as the solvent) were taken into account as the energy corrections calculated using the Gaussian 09 program¹² in terms of the polarizable continuum model (PCM) with the dielectric constant $\epsilon = 2.3741$.

Results and Discussion

Earlier,¹³ nickel intermediates with different composition containing from two to four ligands and their interconversions were considered for the cycloaddition of EA to NBD at the PBE/TZ2P level of theory. It was found that the formation of complexes with four ligands is thermodynamically unfavorable. Considering toluene as the solvent, it was shown that the solvent molecule cannot compete with NBD and EA molecules for the coordination site. The quantum chemical modeling allowed us to establish the mechanism of the reaction under study presented in Scheme 2.

The calculations showed that the two-ligand complex Ni(η^4 -NBD)(η^2 -EA) (**7**) should be considered as the catalytically active species for this reaction. The energy of this species is taken equal to zero. The reaction of complex **7** with EA affords the diolefin intermediate Ni(η^4 -NBD)(η^2 -EA)₂. Due to the different mutual orientation of the coordinated EA molecules, the complex Ni(η^4 -NBD)(η^2 -EA)₂ has ten isomers. The Gibbs free energy of the most stable conformer (**8a**) is 3.4 kcal mol⁻¹ (relative to complex **7** and free EA), and this conformer is common to the routes to the *exo* and *endo* cycloadducts (see Scheme 2, Table 1).

Little energy is required (9 kcal mol⁻¹) to transform complex **8a** into complex **8b**. The distances between the C atoms in the coordinated NBD and EA molecules in this complex are short, which is a prerequisite for the next step of the reaction.

The optimized structures of catalytically active species **7** and intermediates **8a** and **8b** are displayed in Fig. 1; the structures of intermediates **9–14**, in Fig. 2.

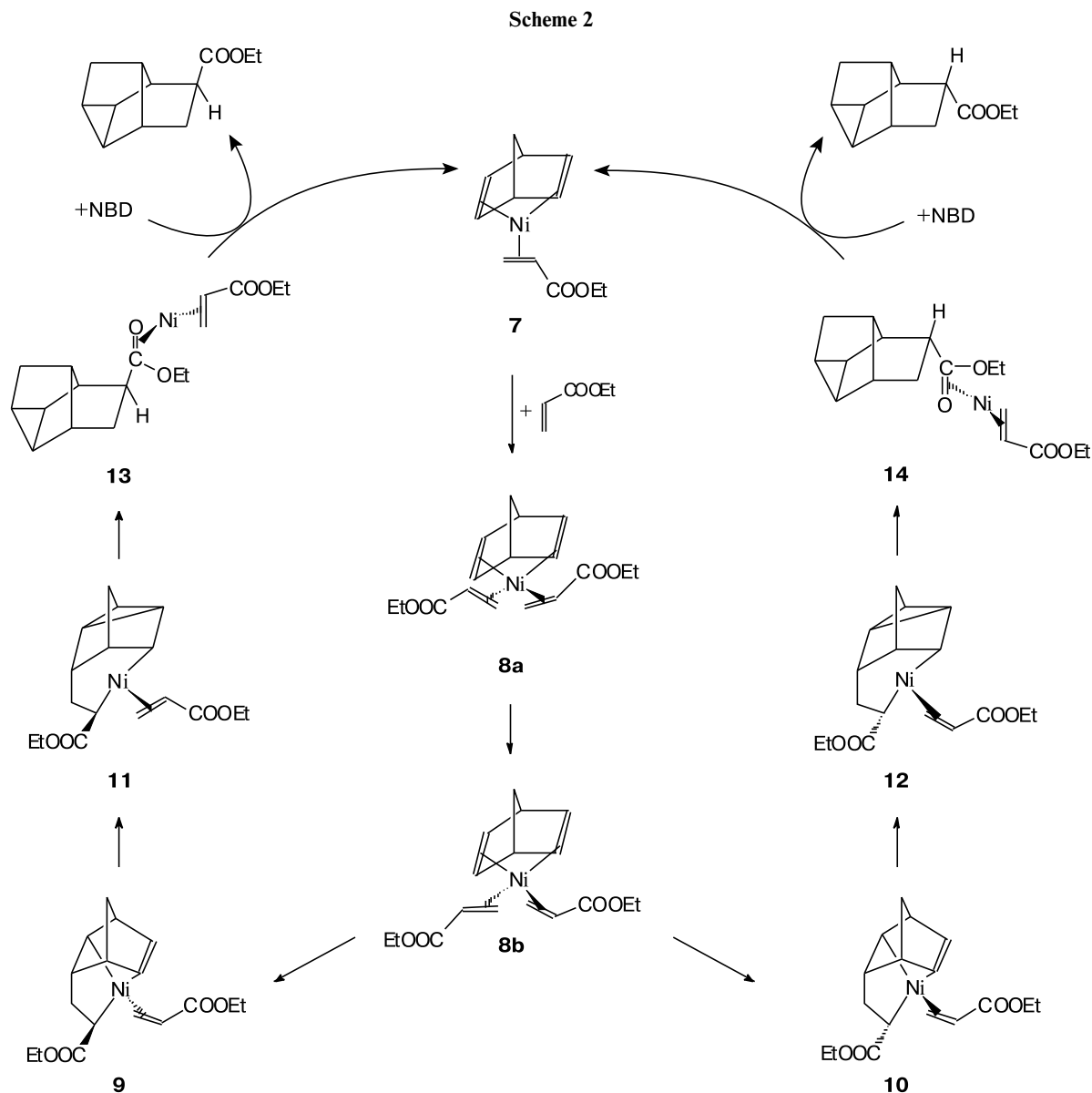


Table 1. Relative free energies (ΔG_{323}) of intermediates and reaction products and the energies of transition states (ΔG_{323}^\ddagger)

Intermediate	ΔG_{323} /kcal mol ⁻¹	TS	ΔG_{323}^\ddagger /kcal mol ⁻¹
7	0	7 → 8a	14.9
8a	3.4	8a → 8b	9.0
8b	6.7	8b → 9	25.6
9	11.8	8b → 10	24.9
10	11.8	9 → 11	21.3
11	7.0	10 → 12	21.4
12	10.4	11 → 13	22.6
13	-1.7	12 → 14	22.2
14	-1.1		

The close arrangement of C atoms in the NBD and EA ligands results in the formation of the first C—C bond. This is a key step because, depending on the type of C atoms coming close to each other, complex **8b** is responsible for the formation of a particular stereoisomer. Thus, the close arrangement of the C(3) and C(6) atoms gives rise to the *exo* cycloadduct, whereas the *endo* cycloadduct is formed if the C(1) and C(8) atoms are closely spaced together. It should be noted that the participation of the terminal C atom of the EA molecule is favorable in both cases, because higher activation barriers have to be overcome in the case of the involvement of other C atoms (for example, C(2) or C(4)). The formation of the first C—C bond is an endothermic step characterized by the activa-

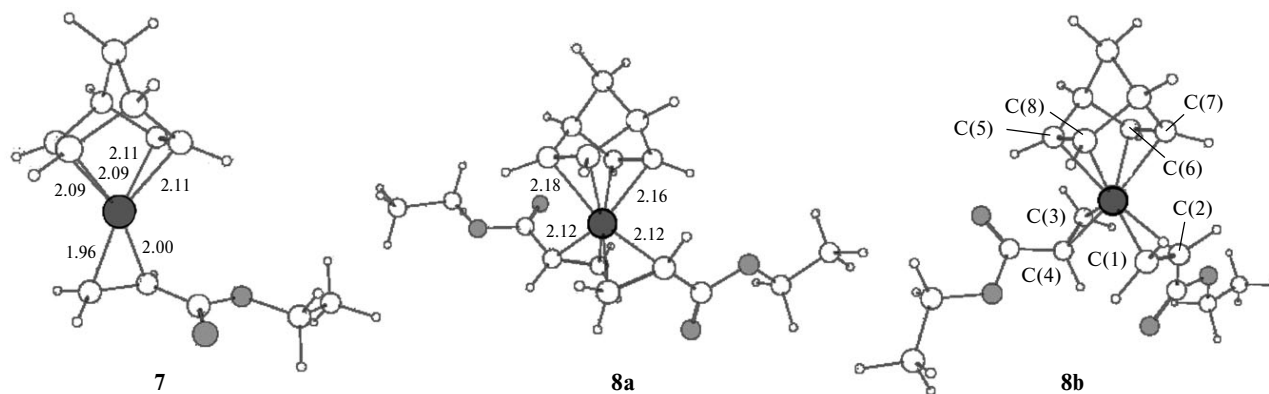


Fig. 1. Structures of the catalytically active species $\text{Ni}(\eta^4\text{-NBD})(\eta^2\text{-EA})$ (**7**) and the diolefin intermediates $\text{Ni}(\eta^4\text{-NBD})(\eta^2\text{-EA})_2$ (**8a** and **8b**) optimized at the PBE/TZ2P level of theory. The interatomic distances are given in Å.

tion barriers of 25.6 and 24.9 kcal mol⁻¹ for the transitions **8b** → **9** and **8b** → **10**, respectively (see Scheme 2, Table 1).

In the next step, the second bond is formed within the NBD moiety between the C(7) and C(8) atoms in complex **9** or between the C(5) and C(6) atoms in complex **10**

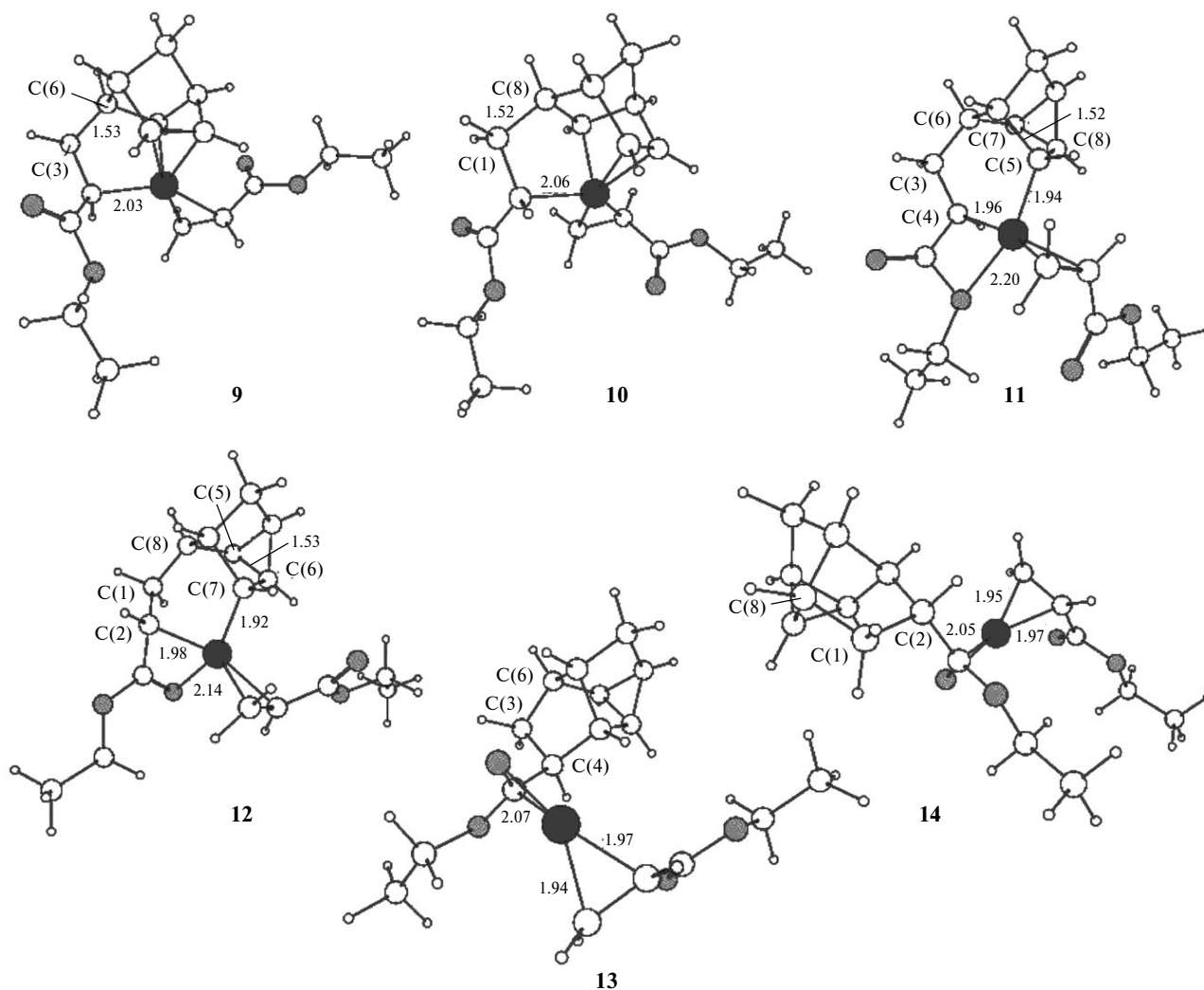


Fig. 2. Structures of intermediates **9**–**14** optimized at the PBE/TZ2P level of theory. The interatomic distances are given in Å.

(see Figs 1 and 2). The formation of these bonds is accompanied by a decrease in the free energies of the systems by 4.8 (**9** → **11**) and 1.4 (**10** → **12**) kcal mol⁻¹, respectively (see Table 1).

The third C—C bond is formed when the C(4) and C(5) atoms in complex **11** or the C(2) and C(7) atoms in complex **12** come close to each other (see Figs 1 and 2). The steps are exothermic, *i.e.*, the free energies of the systems decrease by 8.7 (**11** → **13**) and 11.5 (**12** → **14**) kcal mol⁻¹, respectively (see Table 1).

It should be noted that the above-described sequence of the C—C bond formation is energetically most favorable for the routes to both stereoisomers. In the sequence giving rise to three C—C bonds, the formation of the first C—C bond is characterized by the highest free energy of activation. Consequently, the transitions **8b** → **9** and **8b** → **10** can be considered as the rate-determining steps in the routes to the *exo* and *endo* cycloadducts, respectively (see Table 1).

In the final step of the catalytic cycle, the coordinated cycloadduct molecule in complex **13** (or **14**) is replaced by the NBD molecule, *i.e.*, catalytically active species **7** returns to the system and is ready for the next cycle. The total free energies of formation of the *exo* and *endo* cycloadducts are -27.6 and -27.1 kcal mol⁻¹, respectively. Despite the fact that, according to the results of calculations, the *exo* isomer is thermodynamically slightly more favorable, the experimentally determined concentration of the *endo* isomer is somewhat higher (the ratio of the products is 47 : 53). This may be attributed to the fact that the *endo* isomer is kinetically more favorable because the activation barrier calculated for the rate-determining step of the route to this isomer is 0.7 kcal mol⁻¹ lower than that required for the formation of the *exo* isomer.

Therefore, we modeled for the first time the mechanism of the [2+2+2] cycloaddition of acrylic acid esters to NBD based on the results of quantum chemical calculations for ethyl acrylate. The reaction mechanism involves the formation of the diolefin intermediate common to the routes to both stereoisomers and the sequential formation of three C—C bonds between the NBD and EA ligands. The formation of the first C—C bond is the rate-determining step of the mechanism. Much lesser energies are required to form the next two C—C bonds. According to the mechanism under consideration, the kinetic equation should be first order with respect to acrylate and the catalyst, which is in complete agreement with the experimental data. From the kinetic point of view, the formation of the *endo* cycloadduct is more favorable, which leads to the experimentally observed insignificant predominance of this isomer.

Quantum chemical calculations were carried out using computational facilities of the supercomputer complex installed at the M. V. Lomonosov Moscow State University.

This study was financially supported by the Ministry of Education and Science of the Russian Federation (Agreement 14.V37.21.1658).

References

1. M.-H. Filippini, J. Rodriguez, *Chem. Rev.*, 1999, **99**, 27.
2. US Pat. 5344965, 1994; Appl. No. 110044, CI: C07C 249/00.
3. US Pat. 4 355 194, 1982; Appl. No. 204436, CI: C01L 001/04.
4. M. Lautens, L. Edwards, W. Tam, A. Lough, *J. Am. Chem. Soc.*, 1995, **117**, 10276.
5. D. V. Dmitriev, O. S. Manulik, V. R. Flid, *Kinet. Catal. (Engl. Transl.)*, 2004, **45**, 165 [*Kinet. Katal.*, 2004, **45**, 181].
6. I. E. Efros, D. V. Dmitriev, V. R. Flid, *Kinet. Catal. (Engl. Transl.)*, 2010, **51**, 370 [*Kinet. Katal.*, 2010, **51**, 391].
7. D. N. Laikov, *Chem. Phys. Lett.*, 1997, **281**, 151.
8. J. P. Perdew, K. Burke, M. Ernzerhof, *Phys. Rev. Lett.*, 1996, **77**, 3865.
9. E. M. Evstigneeva, R. S. Shamsiev, V. R. Flid, *Vestn. MITKhT [Fine Chem. Tech.]*, 2006, **1**, 3 (in Russian).
10. R. S. Shamsiev, A. V. Drobyshev, V. R. Flid, *Russ. J. Org. Chem. (Engl. Transl.)*, 2013, **49**, 345 [*Zh. Org. Khim.*, 2013, **49**, 358].
11. R. S. Shamsiev, H. N. Thien, V. R. Flid, *Russ. Chem. Bull. (Int. Ed.)*, 2013, **62**, 1553 [*Izv. Akad. Nauk, Ser. Khim.*, 2013, 1553].
12. M. J. Frisch, G. W. Trucks, H. B. Schlegel, G. E. Scuseria, M. A. Robb, J. R. Cheeseman, G. Scalmani, V. Barone, B. Mennucci, G. A. Petersson, H. Nakatsuji, M. Caricato, X. Li, H. P. Hratchian, A. F. Izmaylov, J. Bloino, G. Zheng, J. L. Sonnenberg, M. Hada, M. Ehara, K. Toyota, R. Fukuda, J. Hasegawa, M. Ishida, T. Nakajima, Y. Honda, O. Kitao, H. Nakai, T. Vreven, J. A. Montgomery, Jr., J. E. Peralta, F. Ogliaro, M. Bearpark, J. J. Heyd, E. Brothers, K. N. Kudin, V. N. Staroverov, R. Kobayashi, J. Normand, K. Raghavachari, A. Rendell, J. C. Burant, S. S. Iyengar, J. Tomasi, M. Cossi, N. Rega, J. M. Millam, M. Klene, J. E. Knox, J. B. Cross, V. Bakken, C. Adamo, J. Jaramillo, R. Gomperts, R. E. Stratmann, O. Yazyev, A. J. Austin, R. Cammi, C. Pomelli, J. W. Ochterski, R. L. Martin, K. Morokuma, V. G. Zakrzewski, G. A. Voth, P. Salvador, J. J. Dannenberg, S. Dapprich, A. D. Daniels, O. Farkas, J. B. Foresman, J. V. Ortiz, J. Cioslowski, D. J. Fox, *Gaussian 09, Revision B.2*, Gaussian, Inc., Wallingford (CT), 2009.
13. R. S. Shamsiev, D. V. Dmitriev, V. R. Flid, *Butlerovskie Soobshcheniya [Butlerov Commun.]*, 2011, **25**, 38 (in Russian).

Received July 8, 2013;
in revised form September 11, 2013